AIDAA
XVI CONGRESSO NAZIONALE AIDAA
24–28 settembre 2001
PALERMO

CONVECTION VELOCITY IN TURBULENT WALL FLOWS

M. QUADRIO[1], P. LUCHINI[2]

[1] *Dipartimento di Ingegneria Aerospaziale Politecnico di Milano*
[2] *Dipartimento di Ingegneria Meccanica Università di Salerno*

ABSTRACT

A direct numerical simulation of the Navier–Stokes equations is used for computing the convection velocity $\mathcal{C}$ of turbulent fluctuations in a plane channel flow. Space-time autocorrelations of the flow variables are analyzed, revealing elongated contour shapes with narrow bands which suggest the convective nature of the flow perturbations. The autocorrelations $R(r_x, r_t)$ of the flow variables as a function of the streamwise and temporal separations are discussed in some detail, in order to describe the effects of the limited extent of the computational domain when (artificial) periodic boundary conditions are used. The convection velocity is then computed, defined as the direction in the r_x, r_t plane where the autocorrelations have their maximum, at vanishingly small time delay. Results concerning the distribution of $\mathcal{C}$ as a function of the distance from the wall are shown and compared with the data available in the literature. It is found that a suitable size of the computational domain is essential for the computation of $\mathcal{C}$.

1. INTRODUCTION

The propagation velocity of perturbations in turbulent wall flows is of fundamental practical importance, given the widespread use of the frozen-equilibrium hypothesis of Taylor, by which one-dimensional power density spectra in wavenumber space are often computed from temporal information, and spatial derivatives are evaluated from time derivatives. Additional physical significance is given to propagation velocity from the increasingly accepted notion of the wall region of turbulent flows as being populated by coherent structures immersed in a random background.

There is a number of experimental works, dating several decades back (see for example [4]), aimed at the experimental evaluation of the convective velocity $\mathcal{C}$ in turbulent wall flows. Accurate measurements of $\mathcal{C}$ were and still are difficult, particularly in the near-wall region. Early measurements showed that convection velocity in the outer region of a boundary layer or channel flow is very near to the local mean velocity; this otherwise reasonable result was implicitly extended to the near-wall region, where measurements

were impossible at that time, and for a long time the convection velocity has been confused with the local mean velocity of the flow, especially for the purpose of applying Taylor's hypothesis.

In more recent years, thanks to the increase in computing power and to the advances in numerical algorithms, the direct numerical simulation (DNS) of the Navier–Stokes equations has become a useful research tool for the study of wall turbulence. Based on the first widely accepted DNS database for the plane turbulent channel flow, computed by [9], some investigation concerning the convection velocity has followed: for example [3] computed the convection velocity of pressure fluctuations at the wall, and [8] first discovered and emphasized the difference between the local mean velocity and convection velocity in the near-wall region.

Due also to the computational difficulties associated in evaluating the convection velocity from the results of a DNS, these works did not have very much follow-up until very recently, where a resurgence of interest on the subject can be noted in the literature: see for example [5]. On the experimental side, a renewed interest has been accompanied by a parallel development of advanced measurement techniques, suitable for very near-wall velocity measurements, as those by [10] and by [7], who are able to measure accurately the streamwise velocity component in low-Reynolds turbulent flows, using specially calibrated hot-wire probes, down to 2 wall units from a solid wall.

The problem of the accurate determination of $\mathcal{C}$ in the near-wall region of a turbulent flow is relatively young, and there are consequently still many open problems. First of all, even if the convection velocity has been computed from DNS data in more than one work, this has been done using always *the same* database, thus claiming for an independent confirmation of the results. Moreover, the effect of the main computational parameters on the computed values of $\mathcal{C}$ has not been addressed yet, in particular the effect of the box dimensions on $\mathcal{C}$ is unknown.

2. THE NUMERICAL APPROACH

The DNS database used in this work is for a turbulent plane channel flow, and is produced by using a recently developed solver of the Navier–Stokes equations for an incompressible fluid, written both in cartesian and cylindrical coordinates. Only the main characteristics of the solver will be illustrated here: additional details can be found in [11].

Our Navier–Stokes solver is based on a mixed discretization: Fourier modes are used for the homogeneous, wall-parallel directions, and high-order finite differences in the wall-normal direction. Finite differences are produced from a fourth-order accurate compact scheme acting on a five-point computational molecule in a variable-spacing mesh. The Navier–Stokes equations are written, similarly to [9], in terms of a scalar equation for the normal component of velocity and a scalar equation for the normal component of vorticity that imitate the Squire decomposition of stability problems, thus achieving the largest computational efficiency when a Fourier discretization is adopted for the horizontal directions. Time advancement of the solution is realized by a commonly used partially implicit approach: nonlinear terms are advanced with an explict scheme (a low-storage, three-substeps, third order Runge-Kutta scheme), and linear terms are advanced with an implicit method (a second order Crank-Nicholson scheme). Finite differences have been preferred to spectral schemes, given their flexibility in dealing with inhomogeneous boundary conditions and easier parallelization. Compact schemes are able to approximate

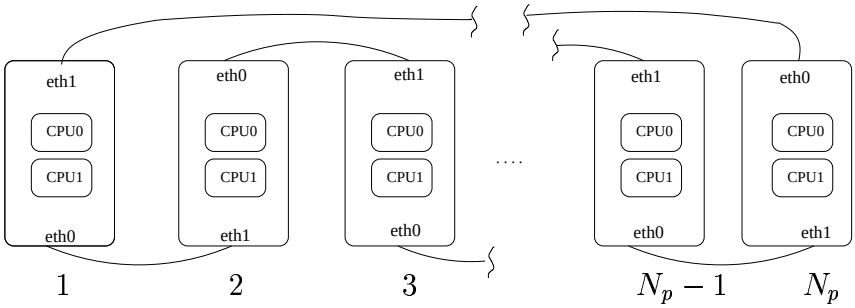

Figure 1: Connection topology of the cluster of PC at DIAPM

a differential operator in a wider frequency range than their non-compact counterparts, thus recovering part of the spectral accuracy.

The computer code is built to be run in parallel, on shared-memory SMP architectures and/or a cluster of distributed-memory computers. We focused the design of the code towards the use of low-cost, commodity hardware, since with commodity (and hence dedicated) machines an unlimited amount of CPU time becomes available with limited financial effort. The code is currently running on a dedicated cluster of 8 SMP Personal Computers, purposely built at the Dipartimento di Ingegneria Aerospaziale del Politecnico di Milano at the cost of approximately 20 million lire. Each node of the cluster is equipped with 2 Pentium III 733-MHz CPU and 256-MB 133-MHz SDRAM; the nodes are connected in a ring with two cheap 100-MBits Fast Ethernet cards each. Thanks to the use of finite differences for the discretization of the normal direction, the parallel algorithm is perfectly suited to a very simple ring topology, schematically illustrated in figure 1, where each machine is directly connected only to the previous machine and to the next. The necessity of a hub or switch is thus eliminated, increasing simplicity, communication bandwidth, and cost-effectiveness at the same time.

The code has been designed with the primary aim of computational efficiency. Its memory requirements are significantly lower that those of similar codes documented in the literature: it saves for example 40% of memory space when compared with the code described in [9], and with the recently optimized code described in [1] and [12].

Efficiency in terms of execution time is more difficult to evaluate, essentially due to lack of complete reference data, but we have estimated that single-processor execution times for a given problem size are fully comparable with those of supercomputer-like processors (slightly more or slightly less, depending on the rank of the supercomputer). Despite the commodity networking hardware, and the use of basic operating system networking services (unix sockets and the TCP/IP protocol) for handling the inter-node communication, the communication time is low enough to have a very moderate impact on efficiency. Figure 2 (left) compares the parallel performances of the code run on the PC cluster, for two problem sizes, with the maximum allowed speedup (less than linear due to small fractions of the code duplicated over all nodes) and with the speedup achieved by [12] on supercomputers after an intensive work of optimization. Using a single processor of one node of the cluster, a full time step for a problem with 129 Fourier modes in longitudinal and spanwise directions, and 129 collocation points in the normal direction requires 50 CPU seconds. Time decreases to approximately 6.5 seconds when the entire cluster is used.

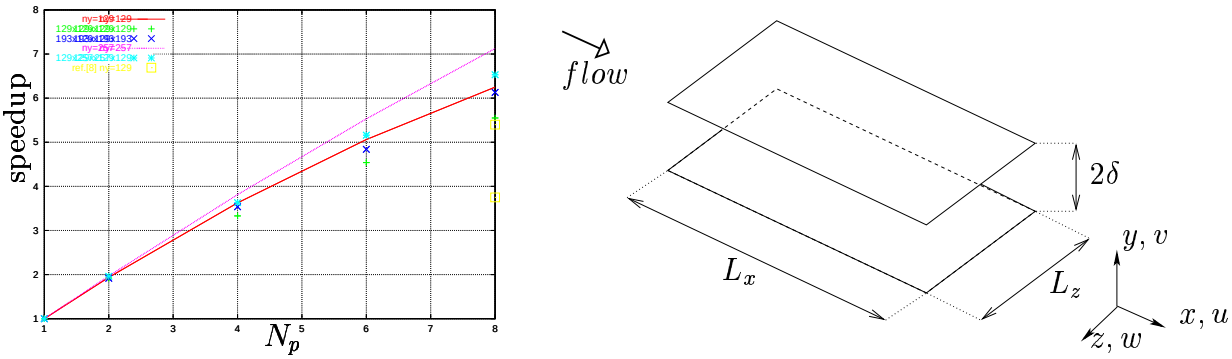

Figure 2: Left: speedup as a function of the number N_P of active nodes of the cluster. Lines without symbols refer to the ideal speedup. Squares are parallel speedups of the code described in [12]. Right: sketch of the computational domain and the coordinate system

3. COMPUTATIONAL PARAMETERS

The cartesian coordinate system used in this work is illustrated in figure 2 (right). The computational domain is a periodic box, with the walls separated by a distance 2δ, with streamwise and spanwise lengths given by $L_x = 2\pi/\alpha_0$ and $L_z = 2\pi/\beta_0$, where α_0 and β_0 are the fundamental wavenumbers in these directions. The reference length δ is taken to be one half of the gap width, and the reference velocity is chosen to be the centerline velocity U_P of a laminar Poiseuille flow with the same flow rate, so that a Reynolds number can be defined as $\mathsf{Re}_P = U_P\delta/\nu$, where ν is the kinematic viscosity of the fluid.

The work concerns two simulations, differing only for the streamwise and spanwise extension of the computational box. Both are at the same Reynolds number of $\mathsf{Re}_P = 4300$, corresponding to a Reynolds number of $\mathsf{Re}_\tau \sim 180$ (based on the friction velocity u_τ).

In the first simulation, the computational parameters are chosen as to match those of [9]: this requires $\alpha_0 = 0.5/\delta$ and $\beta_0 = 1/\delta$, corresponding to $L_x = 4\pi\delta$ and $L_z = 2\pi\delta$. Even the spatial resolution in the homogeneous directions is matched, so that 193 Fouries modes are considered in the streamwise direction, and 161 modes in the spanwise direction. The number of collocation points in the y direction is $N_y = 129$, distributed over an unevenly-spaced mesh.

The second simulation is for a relatively smaller channel, with $\alpha_0 = 1.5/\delta$ and $\beta_0 = 2.5/\delta$, corresponding to $L_x = 4/3\pi\delta$ and $L_z = 4/5\pi\delta$. The spatial resolution has been kept fixed in both cases, so that $N_x = 65$, $N_z = 65$ and $N_y = 129$. In wall units, this corresponds to $\Delta x^+ \sim 12$ and $\Delta z^+ \sim 7$; the spatial resolution in the wall-normal direction varies from $\Delta y^+ \sim 0.8$ near the wall to $\Delta y^+ \sim 4.7$ at the channel centerline.

The numerical time step Δt adopted for advacing the solution has been set to 0.02 in both cases, corresponding to approximately $0.15u_\tau^2/\nu$. The simulations have been run for 600 nondimensional time units for the smaller channel, and for 250 time units for the larger channel. The documentation of these calulations in terms of standard turbulence statistics will be not reported here. Some results from the simulation with the larger channel are reported in [11], and turn out to be essentially identical to those in [9].

In order to compute space-time correlations (from where convection velocities will

be evaluated), two computational strategies are adopted depending on the memory requirements: accumulating the necessary quantities at run time or writing them to disk for further analysis. Owing to the representation adopted, the temporal dependence of the correlation functions is obtained directly, whereas the spatial correlation functions $R(r_x, r_t)$ are obtained by inverse Fourier transforms of spectra $S(\alpha, r_t)$. All correlation data will be shown for a zero separation in the z direction, which amounts to the same as summing the spectrum over all spanwise wavenumbers.

4. SPACE-TIME CORRELATIONS AND DOMAIN SIZE EFFECTS

At a given distance from the wall, and for a given flow variable u, analysis of the two-point autocorrelations $R_{uu}(r_x, r_t)$ as a function of the streamwise separation r_x and the time separation r_t reveals elongated contour shapes concentrated into narrow bands. This is evident, for example, by looking at figure 3 (left), where the autocorrelation function for the components of velocity, at a distance from the wall of 14 wall units, is plotted as a function of the streamwise and temporal separations. The elongation of contours along a preferred direction in the r_x, r_t plane indicates the convective nature of the flow variables, since this direction is associated to a characteristic velocity. Similar plots (not shown here) concerning the two components of wall skin friction exhibit a qualitatively similar behaviour.

The contour plots are obviously periodic in the streamwise direction, where the maximum separation coincides with the streamwise length of the computational domain. The autocorrelation for the streamwise component has the widest contour shapes; the statistics of the u fluctuations in the near-wall region are in fact dominated by the well-known streaky structures, elongated and characterized by a relatively long time scale. R_{vv} on the other hand shows the smallest spatio-temporal scales; the temporal scales associated to R_{ww} at $r_x = 0$ and the spatial scales at $r_t = 0$ are comparably small, but the extension by which R_{ww} remains significantly different from zero in the r_x, r_t plane is as wide as that of R_{uu}.

A cut of these plots at $r_t = 0$ is the usual one-dimensional spectral density function, commonly used ([9]) for verifying *a posteriori* that the extension of the computational domain is adequate to represent an infinite channel notwithstanding the use of periodic boundary conditions. A look at R_{uu} in figure 3 (left) reveals that the correlation decreases down to 0.05 at the middle of the streamwise extent of the computational domain. A similar cut at $r_x = 0$ represents the autocorrelation as a function of the time separation at no streamwise separation, and the value of its first minimum is 0.04. The temporal correlation $R_{uu}(0, r_t)$ allows to estimate the integral longitudinal time scale T_u, given by:

$$T_u = \int_0^\infty R_{uu}(0, r_t) dr_t$$

To date values of T_u computed directly from a DNS are not known. One can estimate, using information both from [9] concernig $R_{uu}(r_x, 0)$ at $y^+ \sim 5$ and from [8] for $\mathcal{C}_u$ at the same y position, a value of $T_u^+ \sim 20$. As the first direct computation of T_u from DNS data, the present work suggests, at the somewhat higher $y^+ = 14$ a value of $T_u^+ \sim 20.7$, obtained integrating $R_{uu}(0, r_t)$ down to its first minimum. In addition the integral time scale can be computed for the other velocity components, obtaining a value of $8u_\tau^2/\nu$ for both T_v and T_w.

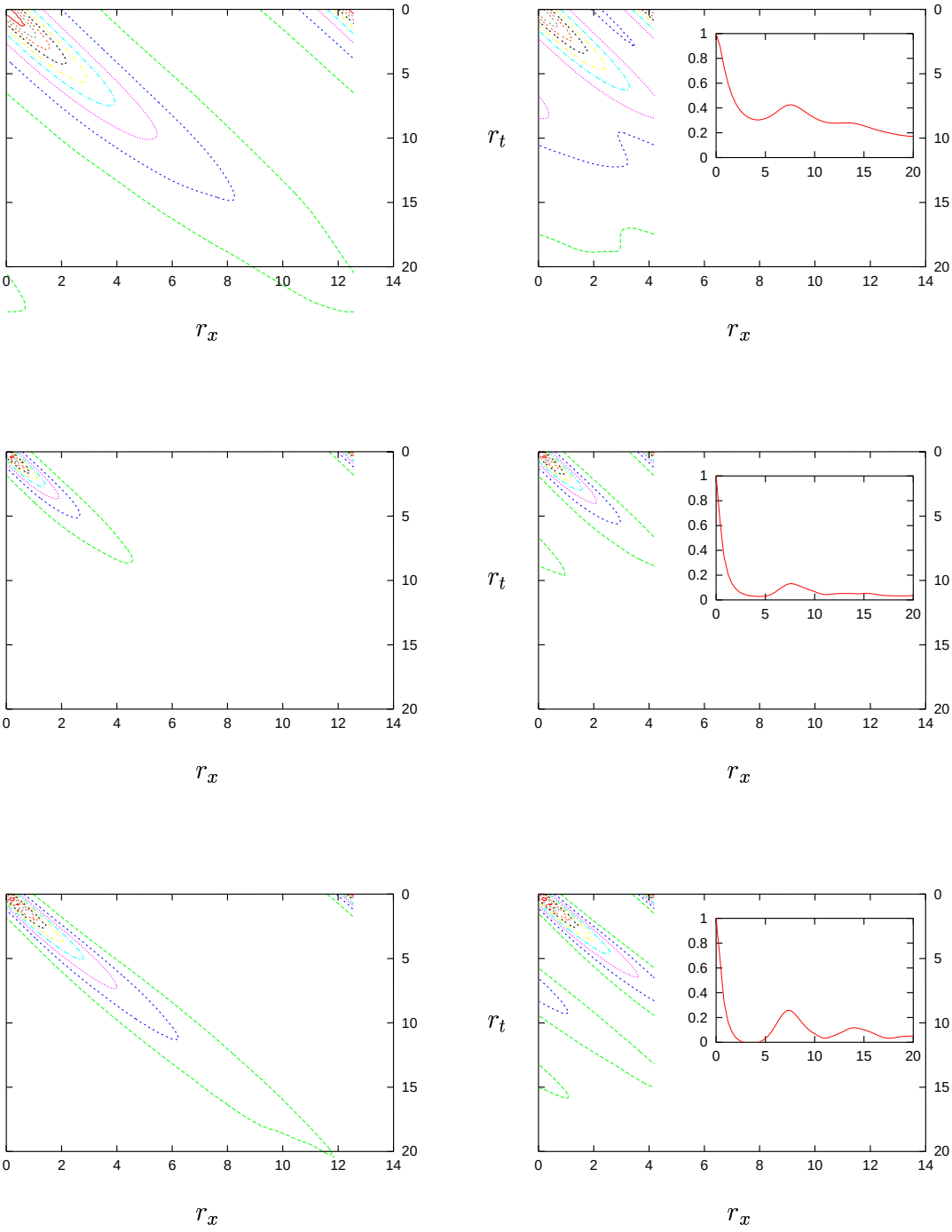

Figure 3: Left: autocorrelation functions for the velocity components at $y^+ = 14$ for the large channel. R_{uu} (top), R_{vv} (center) and R_{ww} (bottom). Contours are from 0.1 to 0.9 by increments of 0.1. Right: same plots, on the same scale, for the smaller channel. Cuts of the autocorrelation functions at zero spatial separation are also shown.

Looking at figure 3 (left), three temporal scales (the same holds true for the spatial scales, related to the temporal scales by the convective nature of the flow) appear to be statistically significant. One is the temporal separation needed for the correlations to decrease to zero; the second is a convective time scale, essentially related to the repeated passages of the turbulence structures convected through the computational box, which becomes evident in the secondary peaks of the correlation $R(0, r_t)$; the third scale is directly related to the "life" of the turbulent structures, and is the separation where the correlations decrease to zero along the direction of their maxima. These scales must be separate enough for the simulation to have physical significance.

Plots like those reported in figure 3 thus allow to judge quantitatively if the longitudinal dimension of the computational domain has been chosen large enough. As an example, in figure 3 (right) the same kind of plots are reported for the second simulation described in § 2, where the dimensions of the computational box, even though still much larger than the minimal flow unit discussed by [6], are reduced in both the homogeneous directions. The time scales are not separate enough here, and spurious, multiple secondary peaks become evident in the time correlations $R(0, r_t)$. The time delay at which correlations peak suggests again the convective nature of the flow, and allows a first rough estimation of the convection velocity, at least when the computational box is short enough for the first peak to be clearly discernible.

5. THE CONVECTION VELOCITY

The convection velocity $\mathcal{C}$, or propagation velocity of perturbations, is defined in this work as the signal propagation velocity ([8]) in planes parallel to the channel walls, which can be deduced from velocity autocorrelation functions. The convection velocity can be deduced also from the analysis of the velocity autospectral density functions, related to autocorrelations by a Fourier transform. These two procedures are not completely equivalent, basically because the statistical error associated with the estimation of the energy spectrum from a finite sample does not decrease with an increasing sample size, whereas the error of the correlation function decreases with the square root of the number of samples [2]. This can be easily confirmed by looking at the very different scatter in the data computed by [5] in their figure 12 for the convection velocity of wall friction and pressure fluctuations, depending wheter spectrum-based or correlation-based definitions are used. Hence in the present work we limit ourselves to consider definitions based on the analysis of autocorrelation functions.

The convection velocity can be defined as the ratio r_x/r_t at which $R(r_x, r_t)$ is maximum, at a fixed time delay or at a fixed streamwise separation. In the former case it is $\mathcal{C} = \mathcal{C}(r_t)$, while in the latter $\mathcal{C} = \mathcal{C}(r_x)$. In their work on convection velocity, [8] decided to compute an overall convection velocity based on the streamwise separation at which the autocorrelation is maximum, choosing somewhat arbitrarily the time delay of $r_t^+ = 18$ ($r_t \sim 2.4$ in the present units).

The direction associated with the convection of the flow variables does not appear to change substantially when different temporal separations are considered, as long as the correlation function remains significantly different from zero. This assumption can be visually checked in figure 3. For definiteness, we decided to compute $\mathcal{C}$ at vanishingly small time delay, i.e. at the time delay corresponding to one numerical time step Δt of the calculation, by looking for the direction where:

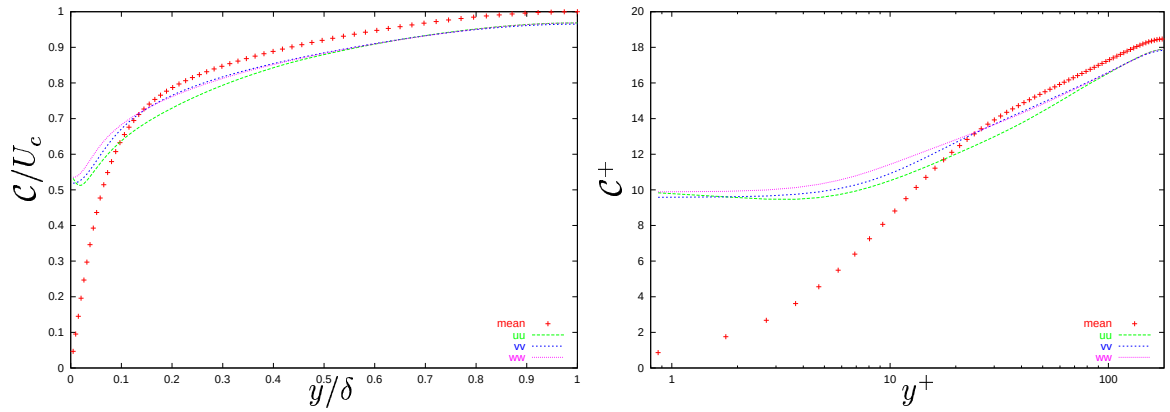

Figure 4: Propagation velocity for the velocity components across the channel, compared to the mean velocity profile: outer scaling (left) and inner scaling (right).

$$\frac{\partial}{\partial r_x} R(r_x, \Delta t) = 0$$

After a Fourier transform, this leads to the relation, valid for example for the u component:

$$\mathcal{C}_u^{n+1} = \mathcal{C}_u^n + \frac{\sum_\alpha S_{uu}(\alpha, \Delta t) i\alpha e^{i\alpha \mathcal{C}_u^n \Delta t}}{\Delta t \sum_\alpha S_{uu}(\alpha, \Delta t)(i\alpha)^2 e^{i\alpha \mathcal{C}_u^n \Delta t}}$$

where $S_{uu}(\alpha, \Delta t)$ is the time average of the autospectral density function for the u component, at a given distance from the wall, at a time separation of $r_t = \Delta t$. From the computational viewpoint, this relation lends itself to a rapidly converging iterative procedure.

The convection velocity, computed according to the preceding formula for the three velocity components, is shown in figure 4 as a function of the distance from the wall, with both external (left) and internal (right) scaling. In the outer part of the channel, the $\mathcal{C}$ evaluated from the three components are almost identical, confirming a sort of statistical isotropy. In this outer region the convection velocity is very similar to the local mean velocity (just slightly lower because of turbulent structures moving on average away from the wall): this qualitatively and quantitatively confirms the whole range of early experimental works, as well as the findings of [8].

In the inner region, the convection velocity is higher than the local mean velocity, and in the near-wall region it is noticeably different from zero, being approximately constant and equal to 0.53 U_c. This is a remarkable result, explained ([8]) by the convective action of outer structures on the flow perturbations near the wall: since flow perturbations at the wall are induced by advecting structures away from the wall, propagation velocity at the wall itself can be high, even if the local mean velocity decreases to zero.

It is possible to note some quantitative differences between the present results and the (few) similar data available in the literature, both from experiments and DNS's. For example the position where $\mathcal{C}$ crosses the mean velocity profile are $y^+ = 18$ for $\mathcal{C}_u$ and $y^+ = 25$ for $\mathcal{C}_v$ and $\mathcal{C}_w$, while [8] report $y^+ = 18$, $y^+ = 20$ and $y^+ = 30$ respectively. Values of $\mathcal{C}^+$ at the wall are between 9.6 and 9.9, very similar to the values by [8], who

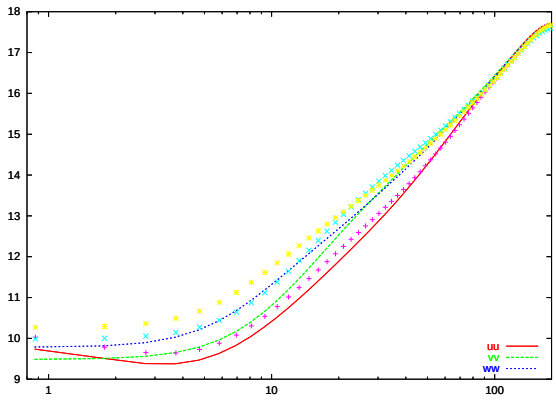

Figure 5: Convection velocity, in inner scaling, computed with large channel data (lines) and small channel data (symbols).

find an approximately constant behaviour in the viscous sublayer. This is consistent also with the results of [5], finding the same value for the convective velocity of shear-stress fluctuations at the wall. Our results indicate that the profiles for $\mathcal{C}_v^+$ and $\mathcal{C}_w^+$ are approximately constant below $y^+ = 6$, but the profile for $\mathcal{C}_u^+$ presents a minimum of 9.47 at $y^+ = 3.5$.

The results of the present work can be then viewed as an independent confirmation of the convection velocity measurements available to date from DNS's. It must be said that the results of the experiments by [10] are quite similar to the present ones, but measure higher values of convective velocity near the wall, with $\mathcal{C}_u^+$ between 11 and 12 at $y^+ = 5$.

Figure 5 reports the distribution of the convection velocity computed from the two DNS's in the larger and smaller channels. We stress again that the smaller channel is not small in absolute terms, since the volume of the computational box is still approximately 10 times larger than that of the minimal flow unit described by [6], which reportedly allows a good calculation of the near-wall turbulence statistics. Below $y^+ = 100$, the calculation of $\mathcal{C}$ is nevertheless affected by the box dimensions down to the channel wall. The convective velocity appears to be overestimated of approximately $0.5 - 1u_\tau$ when computed from the smaller channel data. This means that results from small channel simulations must be considered with care, since they might comparable with results from a simulation with adequate size of the box as far as *some* turbulence statistics are concerned, but not as to others. The sensitivity of convection velocity, computed with an algorithm focusing on the smallest spatio-temporal scales, to the dimensions of the computational box is a rather unexpected result of the present work.

References

[1] K. Alvelius and M. Skote. The performance of a spectral simulation code for turbulence on parallel computers with distributed memory. Technical Report 2000:17, Royal Institute of Technology - Dept. of Mechanics - Stockholm, Sweden, 2000.

[2] J. Bendat and A. Piersol. *Engineering applications of correlatin and spectral analysis.* John Wiley & Sons, 1980.

[3] H. Choi and P. Moin. On the space-time characteristics of wall-pressure fluctuations. *Physics of Fluids A*, 2(8):1450–1460, 1990.

[4] A. Favre, J. Gaviglio, and R. Dumas. Further space-time correlations of velocity in a turbulent boundary layer. *Journal of Fluid Mechanics*, 3:344–356, 1958.

[5] S. Jeon, H. Choi, J. Yoo, and P. Moin. Space-time characteristics of wall shear-stress fuctuations in a low-Reynolds-number channel flow. *Physics of Fluids*, 11(10):3084–3094, 1999.

[6] J. Jimenez and P. Moin. The minimal flow unit in near-wall turbulence. *Journal of Fluid Mechanics*, 225:213–240, 1991.

[7] B. Khoo, Y. Chew, and C. Teo. On near-wall hot-wire measurements. *Experiments in Fluids*, 29(5):448–460, 2000.

[8] J. Kim and F. Hussain. Propagation velocity of perturbations in turbulent channel flow. *Physics of Fluids A*, 5(3):695–706, 1993.

[9] J. Kim, P. Moin, and R. Moser. Turbulence statistics in fully developed channel flow at low Reynolds number. *Journal of Fluid Mechanics*, 177:133–166, 1987.

[10] P. Krogstad, J. Kaspersen, and S. Rimestad. Convection velocities in a turbulent boundary layer. *Physics of Fluids*, 10(4):949–957, 1998.

[11] M. Quadrio and P. Luchini. A 4th order accurate, parallel numerical method for the direct simulation of turbulence in cartesian and cylindrical geometries. In *Proc. of the XV AIMETA Congress on Theoretical and Applied Mechanics*, 2001.

[12] M. Skote. *Studies of turbulent boundary layer flow through direct numerical simulation.* PhD thesis, Royal Institute of Technology Department of Mechanics, 2001.